

A new cosine series antialiasing function and its application to aliasing-free glottal source models for speech and singing synthesis

Hideki Kawahara¹, Ken-Ichi Sakakibara², Hideki Banno³, Masanori Morise⁴, Tomoki Toda⁵
Toshio Irino¹

¹Wakayama University, Japan

²Health Science University of Hokkaido, Japan

³Graduate School of Science and Technology, Meijo University, Japan

⁴Interdisciplinary Graduate School of Medicine and Engineering, University of Yamanashi, Japan

⁵Graduate School of Information Science, Nagoya University, Japan

kawahara@sys.wakayama-u.ac.jp, kis@hoku-iryo-u.ac.jp, banno@meijo-u.ac.jp,
mmorise@yamanashi.ac.jp, tomoki@icts.nagoya-u.ac.jp, irino@sys.wakayama-u.ac.jp

Abstract

We formulated and implemented a procedure to generate aliasing-free excitation source signals based on the Fujisaki-Ljungqvist model. It uses a new antialiasing filter in the continuous time domain followed by an IIR digital filter for response equalization. We introduced a general designing procedure of cosine series to design the new antialiasing function. We also applied this new procedure to revise out previous implementation of the antialiased Fant-Liljencrants model. Combination of these signals and a lattice implementation of time varying vocal tract model provides a reliable and flexible basis to test F0 extractors and source aperiodicity analysis methods. MATLAB implementation of these antialiased excitation source models are available as part of our open source tools for speech science.

Index Terms: antialiasing, glottal source, piece-wise polynomial, piece-wise exponential, cosine series

1. Introduction

Voice quality plays important roles in speech communication, especially in para- and non-linguistic aspects. To test such aspects, it is important to use relevant test stimuli, which sounds natural to listeners, and at the same time, has to be precisely determined and controlled. In addition, it is desirable to be easy to interpret in terms of voice production, as well as auditory perception.

Source filter models with source filter interaction [1] and glottal excitation models [2–9] may provide a practical and useful tool. However, since glottal excitation consists of several types of discontinuity, aliasing introduces spurious signals, which interferes reliable subjective tests. This article introduces a systematic procedure to eliminate aliasing problem by deriving closed form representation of polynomial based on a reference [10]. We also introduce a new set of antialiasing functions using cosine series to keep spurious level around Nyquist frequency low. We will make them accessible by providing MATLAB implementations as well as interactive GUI-based tools [11].

2. Background and related work

One of the authors has been developing a speech analysis, modification and resynthesis framework and related tools [12–14]. It is based on F0-adaptive procedures, which require reliable and precise extraction of F0 and aperiodicity information. Development of such F0 extractors requires dependable ground truth. The aliasing-free L-F model provided the ground truth for developing our new source information analysis framework [15].

Searching aliasing-free glottal source model resulted in one reference [10], which is not directly applicable to antialiasing of the L-F model in two reasons. Firstly, it provides a procedure to antialias polynomials, while the L-F model is a piece-wise exponentials. We have to derive the closed-form representation of the antialiased L-F model by ourselves [16]. Secondly, the reference consisted of typos and missing equations and no sample implementation was not available. In this article, we fixed the procedure and developed executable MATLAB functions. Retrospectively we found BLIT (Band Limited Impulse Train) [17] based methods but found that they are not flexible enough. Literatures on digital representation of analog musical signals also provided aliasing reduction method [18], but they are not directly applicable to glottal excitation models.

Then, there are two important reasons for deriving aliasing-free F-L model. First one is relevance of the model. We found that the L-F model is not necessarily model the actual glottal source behavior, especially extreme voices [19]. Such voices sometimes consists of stronger discontinuities than the L-F model provides. The F-L model provides several different levels of discontinuity and is reported to fit actual speech samples better [6].

Last and the most important reason is that it provides means to generally applicable procedure for antialiasing glottal source models. The F-L model is a piece wise polynomials. The L-F model is a piece wise exponentials. The other popular glottal source models can be represented using both or one of these representations [2–9]. Developing a procedure to make the F-L model aliasing-free provides the necessary piece to attain this goal.

3. F-L model

The F-L model is defined using the following equation in the continuous time domain.

$$E(t) = \begin{cases} A - \frac{2A + R\alpha}{R}t + \frac{A + R\alpha}{R^2}t^2, & 0 < t \leq R \\ \alpha(t - R) + \frac{3B - 2F\alpha}{F^2}(t - R)^2 \\ \quad - \frac{2B - F\alpha}{F^3}(t - R)^3, & R < t \leq W \\ C - \frac{2(C - \beta)}{D}(t - W) \\ \quad + \frac{C - \beta}{D^2}(t - W)^2, & W < t \leq W + D \\ \beta, & W + D < t \leq T \end{cases}, \quad (1)$$

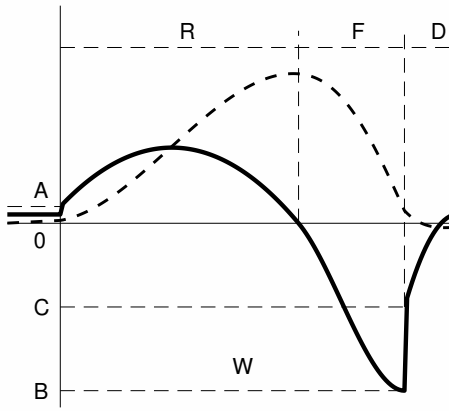


Figure 1: Fujisaki-Ljungqvist model. Glottal air flow $U_g(t)$ (dashed line) and the equivalent excitation signal $E(t)$ (solid line)

where

$$\alpha = \frac{4AR - 6FB}{F^2 - 2R^2} \text{ and } \beta = \frac{CD}{D - 3(T - W)}, \quad (2)$$

Figure 1 shows the F-L model parameters and waveforms. The excitation signal $E(t)$ is a time derivative of glottal flow $U_g(t)$. When the fundamental period T is normalized to one, six model parameters determine the shape. They are A, B, C, R, F, D.

The F-L model is a piece wise polynomial function. Since filtering for antialiasing is a linear operation, antialiasing of the F-L model is solved by adding each antialiased polynomial pulse $p(\tau)$, which is defined in $(0 \leq \tau \leq 1)$ using relevant scaling.

$$p(\tau) = p_0\tau^0 + p_1\tau^1 + \cdots + p_n\tau^n, \quad 0 \leq \tau \leq 1 \quad (3)$$

where scaling is given by $\tau = t/T$.

4. Antialiasing a polynomial pulse

We use the framework proposed by the reference [10]¹. It starts from matrix representation by introducing step functions and antialiasing in the continuos time domain, followed by equalization in the discrete time domain. The simplification and this equalization, as well as application to the F-L model are our contribution.

4.1. Continuous time domain

4.1.1. Matrix form

Let's start from introduction of two step functions $u(\tau)$ and $u(\tau - 1)$. It yields.

$$\begin{aligned} p(\tau) &= p(\tau)u(\tau) - p(\tau)u(\tau - 1) \\ &= \mathbf{p}^T \mathbf{u}_\tau - \mathbf{p}^T \mathbf{B} \mathbf{u}_{\tau-1}, \end{aligned} \quad (4)$$

¹Note that we removed model weighting coefficient w_m in the original reference [10]. It significantly simplifies the following discussion.

where \mathbf{B} is a lower triangular matrix defined below.

$$\mathbf{B} = \begin{bmatrix} b_{00} & 0 & \cdots & 0 \\ b_{10} & b_{11} & \ddots & \vdots \\ \vdots & \ddots & \ddots & 0 \\ b_{n0} & b_{n1} & \cdots & b_{nn} \end{bmatrix}, \quad (5)$$

the coefficient $b_{nk} = n!/(k!(n - k)!)$ is a binomial coefficient and \mathbf{p} , \mathbf{u}_τ and $\mathbf{u}_{\tau-1}$ are vectors defined below.

$$\mathbf{p} = \begin{bmatrix} p_0 \\ p_1 \\ \vdots \\ p_n \end{bmatrix}, \mathbf{u}_\tau = \begin{bmatrix} \tau^0 u(\tau) \\ \tau^1 u(\tau) \\ \vdots \\ \tau^n u(\tau) \end{bmatrix}, \mathbf{u}_{\tau-1} = \begin{bmatrix} (\tau - 1)^0 u(\tau - 1) \\ (\tau - 1)^1 u(\tau - 1) \\ \vdots \\ (\tau - 1)^n u(\tau - 1) \end{bmatrix} \quad (6)$$

4.1.2. Antialiasing using a cosine series

The antialiased filtered pulse $p_h(\tau)$ has the following form.

$$p_h(\tau) = h(\tau) * \{p(\tau)u(\tau) - p(\tau)u(\tau - 1)\}, \quad (7)$$

where $h * u$ represents convolution of h and u . Then, convolution is a linear operation, it yields the following.

$$p_h(\tau) = \mathbf{p}^T \mathbf{h}_\tau - \mathbf{p}^T \mathbf{B} \mathbf{h}_{\tau-1}, \quad (8)$$

where \mathbf{h}_τ and $\mathbf{h}_{\tau-1}$ represent vectors defined below.

$$\mathbf{h}_\tau = \begin{bmatrix} h(\tau) * \tau^0 u(\tau) \\ h(\tau) * \tau^1 u(\tau) \\ \vdots \\ h(\tau) * \tau^n u(\tau) \end{bmatrix}, \mathbf{h}_{\tau-1} = \begin{bmatrix} h(\tau) * (\tau - 1)^0 u(\tau - 1) \\ h(\tau) * (\tau - 1)^1 u(\tau - 1) \\ \vdots \\ h(\tau) * (\tau - 1)^n u(\tau - 1) \end{bmatrix}. \quad (9)$$

Equation provides the antialiased signal to be discretized. We use the following cosine series for antialiasing filter response $h(t)$.

$$h(t) = \sum_{k=0}^m h_k \cos\left(\frac{k\pi t}{t_w}\right), \quad -t_w < t \leq t_w, \quad (10)$$

where m represents the exponent of the highest order term and t_w represents the length of the filer, which is determined according to the sampling frequency.

Assigning specific values to coefficients h_k determines \mathbf{h}_τ and $\mathbf{h}_{\tau-1}$. We derive the closed form representation of Equation and then discretize it. The equation to determine \mathbf{h}_τ and $\mathbf{h}_{\tau-1}$ is the following. The next step is to determine the matrices \mathbf{C} , \mathbf{S} , \mathbf{U} , and \mathbf{V} , with constant coefficients.

$$\mathbf{h}_t = \begin{cases} 0, & t \leq -t_w \\ \mathbf{C} \mathbf{c}_t + \mathbf{S} \mathbf{s}_t + \mathbf{U} \mathbf{t}_{n+1}, & -t_w < t \leq t_w \\ \mathbf{V} \mathbf{t}_n, & t_w < t \end{cases} \quad (11)$$

$$\mathbf{h}_{t-1} = \mathbf{C} \mathbf{c}_{t-1} + \mathbf{S} \mathbf{s}_{t-1} + \mathbf{U} \mathbf{d}_{n+1}, \quad 1 - t_w < t \leq 1 + t_w, \quad (12)$$

where each element of vectors \mathbf{c}_t , \mathbf{s}_t , \mathbf{t}_{n+1} and \mathbf{t}_n are defined below, where $(\mathbf{c}_t)_k$ represents the k -th element of \mathbf{c}_t .

$$(\mathbf{c}_t)_k = \cos\left(\frac{k\pi t}{t_w}\right), \quad (\mathbf{s}_t)_k = \sin\left(\frac{k\pi t}{t_w}\right), \quad (\mathbf{t}_n)_k = t^{k-1}, \quad (13)$$

and vectors \mathbf{c}_{t-1} , \mathbf{s}_{t-1} and \mathbf{d}_{n+1} are defined below.

$$(\mathbf{c}_{t-1})_k = \cos\left(\frac{k\pi(t-1)}{t_w}\right), \quad (\mathbf{s}_{t-1})_k = \sin\left(\frac{k\pi(t-1)}{t_w}\right)$$

$$(\mathbf{d}_{n+1})_k = (t-1)^{k-1}. \quad (14)$$

4.1.3. Recursive determination of coefficients

The recursion uses the following continuity constraints and initial values. The continuity gives the following.

$$\mathbf{Cc}_t + \mathbf{Ss}_t + \mathbf{Ut}_{n+1} = 0 \quad t = -t_w \quad (15)$$

$$\mathbf{Cc}_t + \mathbf{Ss}_t + \mathbf{Ut}_{n+1} = \mathbf{Vt}_n \quad t = t_w. \quad (16)$$

The initial condition is for the first row of the matrices, where m represents the highest exponent of the selected cosine series antialiasing function. In the following equation, $\mathbf{C}_{r,k}$ represents the element on r -th row and k -th column.

$$\begin{aligned} \mathbf{C}_{0,k} &= 0, \quad 1 \leq k \leq m, \\ \mathbf{S}_{0,k} &= \left(\frac{t_w}{k\pi} \right) h_k, \quad 1 \leq k \leq m, \\ \mathbf{U}_{0,1} &= h_0, \\ \mathbf{U}_{0,k} &= 0, \quad 1 < k \leq n+1, \\ \mathbf{V}_{0,0} &= 1, \quad (\text{This is missing in [10].}), \\ \mathbf{V}_{0,k} &= 0, \quad 1 \leq k \leq n, \end{aligned} \quad (17)$$

For $r = 1$ through $r = n$ the following recursion determines the coefficients.

$$\begin{aligned} \mathbf{C}_{r,k} &= - \left(\frac{rt_w}{k\pi} \right) \mathbf{S}_{r-1,k}, \quad 1 \leq k \leq m, \\ \mathbf{S}_{r,k} &= \left(\frac{rt_w}{k\pi} \right) \mathbf{C}_{r-1,k}, \quad 1 \leq k \leq m, \\ \mathbf{U}_{r,k} &= \left(\frac{r}{k} \right) \mathbf{U}_{r-1,k-1}, \quad 1 \leq k \leq n+1, \\ \mathbf{U}_{r,0} &= - \sum_{k=1}^{n+1} (-t_w)^k \mathbf{U}_{r,k} - \sum_{k=1}^m (-1)^k \mathbf{C}_{r,k}, \\ \mathbf{V}_{r,k} &= \left(\frac{r}{k} \right) \mathbf{V}_{r-1,k-1}, \quad 1 \leq k \leq n, \\ \mathbf{V}_{r,0} &= \sum_{k=0}^{n+1} (t_w)^k \mathbf{U}_{r,k} + \sum_{k=1}^m (-1)^k \mathbf{C}_{r,k} - \sum_{k=1}^n (t_w)^k \mathbf{V}_{r,k}, \end{aligned} \quad (18)$$

where the fourth and sixth lines were placed in a confusing manner in the reference [10]. Also the reference has typo in Eq. 17 for defining $\mathbf{U}_{0,1}$.

4.1.4. Closed form representation

The following equation provides the antialiased polynomial value at given t .

$$p_h(t) = \begin{cases} \mathbf{c}_0 \mathbf{c}_t + \mathbf{s}_0 \mathbf{s}_t + \mathbf{u}_0 \mathbf{t}_{n+1} & \mathcal{Q}_1(t) \\ \mathbf{v} \mathbf{t}_n & \mathcal{Q}_2(t) \\ \mathbf{c}_0 \mathbf{c}_t + \mathbf{s}_0 \mathbf{s}_t + \mathbf{u}_0 \mathbf{t}_{n+1} \\ \quad - (\mathbf{c}_1 \mathbf{c}_{t-1} + \mathbf{s}_1 \mathbf{s}_{t-1} + \mathbf{u}_1 \mathbf{d}_{n+1}) & \mathcal{Q}_3(t) \\ \mathbf{v} \mathbf{t}_n - (\mathbf{c}_1 \mathbf{c}_{t-1} + \mathbf{s}_1 \mathbf{s}_{t-1} + \mathbf{u}_1 \mathbf{d}_{n+1}) & \mathcal{Q}_4(t) \end{cases} \quad (19)$$

where

$$\begin{aligned} \mathcal{Q}_1(t) &= \{-t_w < t \leq t_w \wedge t \leq 1 - t_w\} \\ \mathcal{Q}_2(t) &= \{t_w < t \leq 1 - t_w\} \\ \mathcal{Q}_3(t) &= \{1 - t_w < t \leq t_w\} \\ \mathcal{Q}_4(t) &= \{1 - t_w < t \leq 1 + t_w \wedge t_w < t\} \end{aligned}, \quad (20)$$

where \wedge represents logical AND. Note that we have to refine conditions given in the reference [10] to make this procedure to work properly. Coefficient vectors are defined as follows

$$\begin{aligned} \mathbf{c}_0 &= \mathbf{p}^T \mathbf{C}, & \mathbf{s}_0 &= \mathbf{p}^T \mathbf{S}, & \mathbf{u}_0 &= \mathbf{p}^T \mathbf{U}, & \mathbf{v} &= \mathbf{p}^T \mathbf{V}, \\ \mathbf{c}_1 &= \mathbf{p}^T \mathbf{BC}, & \mathbf{s}_1 &= \mathbf{p}^T \mathbf{BS}, & \mathbf{u}_1 &= \mathbf{p}^T \mathbf{BU} \end{aligned} \quad (21)$$

5. Antialiasing function

We introduce two new cosine series antialiasing functions here. Because of infinite frequency range of the glottal excitation models, which have discontinuities, commonly used time windowing functions with 6 dB/oct sidelobe decay [20–23] introduces significant spurious due to aliasing. In our previous derivation, we used one of Nuttall's window [24] for the antialiasing function. It has the following coefficient.

$$\{h_k\}_{k=0}^3 = \{0.338946, 0.481973, 0.161054, 0.018027\} \quad (22)$$

The maximum side lobe level is -82.6 dB and the decay speed of side lobes is 30 dB/oct. This decay rate was not steep enough to suppress spurious component around F0 and sidelobe level is not low enough to suppress spurious component around Nyquist frequency. The other windows listed in [24] cannot solve both issues at the same time.

5.1. Designing procedure

Using the similar process used in [24], we design new set of windows to satisfy both sidelobe level and decay conditions. We use cosine series to design the antialiasing function. The element of the cosine series has the following form.

$$\psi_k(t) = \begin{cases} \cos \left(\frac{k\pi t}{t_w} \right), & -t_w \leq t \leq t_w \\ 0 & |t| > t_w \end{cases}. \quad (23)$$

For the designed function to behave properly for antialiasing, following conditions have to be satisfied. Note that the odd ordered derivatives are always zero for $t = \pm t_w$.

Sum of coefficients to be one This determines the height of the function at the origin. For simplicity, we set it one.

Level at the end point to be zero The function to be continuous at the end point.

Derivatives at the end point to be zero Depending on the required slope, derivatives at end point has to be equal to zero. For decay rate $6 + (12 \times P)$ dB/oct, derivatives up to the order $2P$ are zero.

These conditions are summarized by the following set of equations.

$$h(0) = \sum_{k=0}^m h_k = 1 \quad (24)$$

$$h(\pm t_w) = \sum_{k=0}^m (-1)^k k^0 h_k = 0 \quad (25)$$

$$\left. \frac{d^{2p} h(t)}{dt^{2p}} \right|_{t=\pm t_w} = \sum_{k=0}^m (-1)^k k^{2p} h_k = 0, \quad p = 1, \dots, P \quad (26)$$

Once the desired decay is decided, it provides $P + 2$ conditions. If the number of coefficients of the cosine series is equal to $P + 2$, there is no room for adjustment. By adding one adjustable coefficient, we can control the sidelobe level. It yields the following equation.

$$\mathbf{q} = \mathbf{Rg}, \quad (27)$$

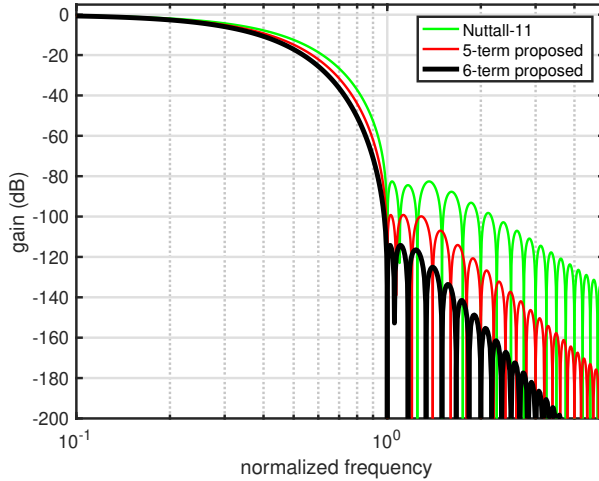


Figure 2: Gain of new antialiasing functions and the Nuttall-11 window.

where

$$R = \begin{bmatrix} 1 & 1 & \cdots & 1 & 1 & 1 \\ 1 & -1 & \cdots & (-1)^k k^0 & \cdots & (-1)^m m^0 \\ 0 & -1 & \cdots & (-1)^k k^2 & \cdots & (-1)^m m^2 \\ \vdots & \vdots & \vdots & \vdots & \vdots & \vdots \\ 0 & -1 & \cdots & (-1)^k k^{2p} & \cdots & (-1)^m m^{2p} \\ \vdots & \vdots & \vdots & \vdots & \vdots & \vdots \\ 0 & -1 & \cdots & (-1)^k k^{2P} & \cdots & (-1)^m m^{2P} \\ 1 & 0 & \cdots & 0 & \cdots & 0 \end{bmatrix} \quad (28)$$

$$\mathbf{q} = [1, 0, \dots, 0, q_0]^T. \quad (29)$$

The solution is given by:

$$\mathbf{g} = R^{-1} \mathbf{q}, \quad (30)$$

where elements of \mathbf{g} provides coefficients of cosine series. Designing antialiasing function is to tune the parameter q_0 to minimize the target cost. This time, the target is the level of the maximum sidelobe level. For 36 dB/oct decay, 5-term cosine series is designed. For 48 dB/oct decay, 6-term cosine series is designed.

Numerical optimization yielded the following coefficients.

$$\{h_k\}_{k=0}^4 = \{0.29405, 0.45399, 0.20226, 0.04601, 0.00369\} \quad (31)$$

$$\{h_k\}_{k=0}^5 = \{0.26250000, 0.42656250, 0.22500000, 0.07265625, 0.01250000, 0.00078125\}, \quad (32)$$

Substituting these coefficients to Eq. 21 provides antialiased F-L model in the continuous time domain. The half of the window length t_w is set to make the first zero of the frequency domain representation coincides to $f_s/2$, where f_s represents the sampling frequency.

Figure 2 shows gain of these new functions and the Nuttall window, which was used for the aliasing-free L-F model [16]. The 5-term function has -99.2 dB maximum sidelobe level with 30 dB/oct decay. The 6-term function has -114.1 dB maximum sidelobe level with 42 dB/oct decay. We decided to use the 6-term function afterwards.

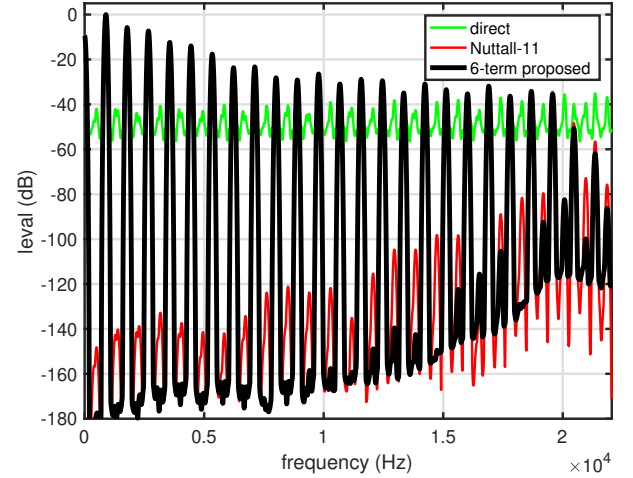


Figure 3: Power spectra of direct and two antialiased signals of the Fujisaki-Ljungqvist model. F_0 is set to 887 Hz to make spurious due to aliasing salient.

5.2. Discrete time domain

Final stage is processed in the discrete time domain. It is equalization.

5.2.1. Equalization

The designed antialiasing functions introduce severe attenuation around Nyquist frequency. In our antialiased L-F model, an FIR equalizer was designed to compensate for this attenuation [16]. We use a simple IIR filter with six poles in this F-L model and found that it equalizes this attenuation effectively. A sample implementation makes equalized gain deviation from the FIR version within ± 0.2 dB from 0 to 16 kHz for 44100 Hz sampling.

6. Antialiased F-L model

Calculating the antialiased F-L model output is to calculate each antialiased polynomial and sum together. Discretization is to calculate the antialiased F-L model value at each sampling instance. Finally, applying the discrete time IIR equalizer to the discretized samples provides the discrete signal of the antialiased F-L model.

6.1. Examples

We implemented this procedure using MATLAB and prepared several high-level API. One function generates an excitation source signal using given F_0 trajectory and time varying F-L model parameter set $A(t), B(t), C(t), R(t), F(t)$ and $D(t)$.

Figure 3 shows a power spectra of the F-L model outputs. Direct discretization generates aliasing noise around -60 dB from the peak harmonics level. Noise level of the final equalization around the fundamental component is about -180 dB when using the 6-term proposed function. Antialiasing using Nuttall-11 window introduces about 20 dB higher spurious level. (Note the noise level using `nuttallwin` of MATLAB as antialiasing is about -120 dB.)

6.2. Revision of antialiased L-F model

We revised our previous antialiased L-F model [16] using new 6-term cosine series and 6 pole IIR equalizer. We also reformulated algorithm using element function $\varphi_k(t) = I_1 + I_2 + I_3$ as

a building block to define the antialiased and normalized complex exponential pulse $p_h(t)$.

$$p_h(t) = \frac{1}{2t_w h_0} \sum_{k=0}^6 h_k \varphi_k(t), \quad (33)$$

where $\{h_k\}_{k=0}^6$ is given by Eq. 32. The factor $2t_w h_0$ is for gain normalization. For each $k > 0$, explicit form is given below.

$$I_1 = \frac{k\alpha \sin(k\alpha t) - \beta \cos(k\alpha t) + (-1)^k \beta \exp(\beta(t_w+t))}{k^2 \alpha^2 + \beta^2} \quad (34)$$

$$I_2 = \frac{(-1)^k \beta \exp(\beta t) (\exp(\beta t_w) - \exp(-\beta t_w))}{k^2 \alpha^2 + \beta^2} \quad (35)$$

$$I_3 = \frac{1}{k^2 \alpha^2 + \beta^2} \{k\alpha \exp(\beta) \sin(k\alpha(t-1)) - \beta \exp(\beta) \cos(k\alpha(t-1)) + (-1)^k \beta \exp(\beta(t_w+t))\}, \quad (36)$$

where $\alpha = \pi/t_w$. Functions I_1 , I_2 and I_3 are defined in $(-t_w, t_w)$, $(t_w, 1+t_w)$ and $[1-t_w, 1+t_w)$ respectively. They are 0 outside. Note that the second interval overlaps with the third one. The constant β can be a complex number depending on the piece. For example, the first piece of the L-F model, β is a complex number and $\Im[p_h(t)]$ provides the antialiased result. For $k = 0$, the 0-th order antialiased polynomial pulse is applicable.

7. Conclusions

We formulated and implemented a procedure to generate aliasing-free glottal source model output. We antialiased the Fujisaki-Ljungqvist model using a newly designed cosine series antialiasing function, followed by an IIR digital equalizer. We also revised our antialiased L-F model using the 6-term cosine series and the IIR equalizer. The proposed procedure is general enough to be applicable to other glottal source models and any signal models consisting of polynomial and complex exponential segments. These antialiased models are made open access MATLAB procedures with interactive GUI tools for education and research of speech science [11]. The antialiased glottal excitation signals also provide reliable and flexible means to test F0 extractors and source aperiodicity analysis procedures.

8. Acknowledgements

This work was supported by JSPS KAKENHI Grant Numbers JP15H03207, JP15H02726 and JP16K12464.

9. References

- [1] I. R. Titze, "Nonlinear source-filter coupling in phonation: Theory," *J. Acoust. Soc. Am.*, vol. 123, no. 5, pp. 2733–2749, may 2008.
- [2] A. E. Rosenberg, "Effect of glottal pulse shape on the quality of natural vowels," *The Journal of the Acoustical Society of America*, vol. 49, no. 2B, pp. 583–590, 1971.
- [3] P. Hedelin, "A glottal lpc-vocoder," in *Acoustics, Speech, and Signal Processing, IEEE International Conference on ICASSP'84*, vol. 9. IEEE, 1984, pp. 21–24.
- [4] G. Fant, J. Liljencrants, and Q.-g. Lin, "A four-parameter model of glottal flow," *STL-QPSR*, vol. 4, no. 1985, pp. 1–13, 1985.
- [5] H. Fujisaki and M. Ljungqvist, "Proposal and evaluation of models for the glottal source waveform," in *ICASSP 1986*, Tokyo, 1986, pp. 1605–1608.
- [6] ———, "Estimation of voice source and vocal tract parameters based on ARMA analysis and a model for the glottal source waveform," in *ICASSP 1987*, 1987, pp. 637–640.
- [7] D. H. Klatt and L. C. Klatt, "Analysis, synthesis, and perception of voice quality variations among female and male talkers," *The Journal of the Acoustical Society of America*, vol. 87, no. 2, pp. 820–857, 1990.
- [8] Y.-L. Shue and A. Alwan, "A new voice source model based on high-speed imaging and its application to voice source estimation," in *Acoustics Speech and Signal Processing (ICASSP), 2010 IEEE International Conference on*. IEEE, 2010, pp. 5134–5137.
- [9] P. Alku, "Glottal inverse filtering analysis of human voice production - A review of estimation and parameterization methods of the glottal excitation and their applications," *Sadhana - Academy Proceedings in Engineering Sciences*, vol. 36, no. October, pp. 623–650, 2011.
- [10] P. H. Milenovic, "Voice source model for continuous control of pitch period," *The Journal of the Acoustical Society of America*, vol. 93, no. 2, pp. 1087–1096, 1993.
- [11] H. Kawahara, "SparkNG: Interactive MATLAB tools for introduction to speech production, perception and processing fundamentals and application of the aliasing-free L-F model component," in *Interspeech 2016*, San Francisco, 2016.
- [12] H. Kawahara, I. Masuda-Katsuse, and A. de Cheveigne, "Restructuring speech representations using a pitch-adaptive time-frequency smoothing and an instantaneous-frequency-based F0 extraction," *Speech Communication*, vol. 27, no. 3-4, pp. 187–207, 1999.
- [13] H. Kawahara, M. Morise, T. Takahashi, R. Nisimura, T. Irino, and H. Banno, "TANDEM-STRAIGHT: A temporally stable power spectral representation for periodic signals and applications to interference-free spectrum, F0 and aperiodicity estimation," in *ICASSP 2008*, Las Vegas, 2008, pp. 3933–3936.
- [14] H. Kawahara, M. Morise, Banno, and V. G. Skuk, "Temporally variable multi-aspect N-way morphing based on interference-free speech representations," in *ASPIPA ASC 2013*, 2013, p. 0S28.02.
- [15] H. Kawahara, Y. Agiomyrgiannakis, and H. Zen, "Using instantaneous frequency and aperiodicity detection to estimate F0 for high-quality speech synthesis," *arXiv preprint arXiv:1605.07809*, 2016. [Online]. Available: <http://arxiv.org/abs/1605.07809>
- [16] H. Kawahara, K.-I. Sakakibara, H. Banno, M. Morise, T. Toda, and T. Irino, "Aliasing-free implementation of discrete-time glottal source models and their applications to speech synthesis and F0 extractor evaluation," in *2015 Asia-Pacific Signal and Information Processing Association Annual Summit and Conference (APSIPA)*. Hong Kong: IEEE, dec 2015, pp. 520–529. [Online]. Available: <http://ieeexplore.ieee.org/lpdocs/epic03/wrapper.htm?arnumber=7415325>
- [17] T. Stilson and J. Smith, "Alias-free digital synthesis of classic analog waveforms," in *Proc. International Computer Music Conference*, 1996, pp. 332–335.
- [18] V. Valimaki, "Discrete-time synthesis of the sawtooth waveform with reduced aliasing," *IEEE Signal Processing Letters*, vol. 12, no. 3, pp. 214–217, March 2005.
- [19] K.-I. Sakakibara, H. Imagawa, H. Yokonishi, M. Kimura, and N. Tayama, "Physiological observations and synthesis of subharmonic voices," in *Asia-Pacific Signal and Information Processing Association Annual Summit and Conference*, 2011, pp. 1079–1085.
- [20] D. Slepian and H. O. Pollak, "Prolate spheroidal wave functions, Fourier analysis and uncertainty-I," *Bell System Technical Journal*, vol. 40, no. 1, pp. 43–63, 1961.
- [21] D. Slepian, "Prolate spheroidal wave functions, Fourier analysis, and uncertainty-V: The discrete case," *Bell System Technical Journal*, vol. 57, no. 5, pp. 1371–1430, 1978.
- [22] F. J. Harris, "On the use of windows for harmonic analysis with the discrete Fourier transform," *Proceedings of the IEEE*, vol. 66, no. 1, pp. 51–83, 1978.
- [23] J. Kaiser and R. W. Schafer, "On the use of the L0-sinh window for spectrum analysis," *Acoustics, Speech and Signal Processing, IEEE Transactions on*, vol. 28, no. 1, pp. 105–107, 1980.

[24] A. H. Nuttall, "Some windows with very good sidelobe behavior," *IEEE Trans. Audio Speech and Signal Processing*, vol. 29, no. 1, pp. 84–91, 1981.

[25] D. G. Childers and C. Ahn, "Modeling the glottal volumevelocity waveform for three voice types," *The Journal of the Acoustical Society of America*, vol. 97, no. 1, pp. 505–519, 1995.

A. Supplement

This draft is submitted to Interspeech 2017. This appendix provides materials, which were dropped due to available space.

A.1. Test signals

We used frequency modulated F0 trajectory $f_{0i}(t)$ for generating figures shown in this article. The following equation provides the details.

$$f_{0i}(t) = f_{base} 2^{\left(\frac{f_d}{1200} \sin(2\pi f_m t)\right)}, \quad (37)$$

where f_d determines the depth of the vibrato in terms of musical cent and f_m determines the rate of vibrato. We used $f_d = 6$ (cent) and $f_m = 5.2$ (Hz) for generating figures. The F-L model parameters $\{A, B, C, R, F, D\}$ were set as follows.

$$\{A, B, C, R, F, D\} = \{0.2, -1, -0.6, 0.48, 0.15, 0.12\}. \quad (38)$$

We also generated test signals using the antialiased L-F model. The same frequency modulated F0 trajectory was used. The L-F model parameters $\{t_p, t_e, t_a, t_c\}$ were set as follows.

$$\{t_p, t_e, t_a, t_c\} = \{0.4134, 0.5530, 0.0041, 0.5817\}, \quad (39)$$

where the specific values are average value of modal voices reported in the reference [25].

A.2. Spectrogram of F-L model

Figure 4 shows spectrogram of the generated excitation source signals using direct discretization, Nuttall-11 window, and the proposed 6-term cosine series. The spectrum slices in Fig. 3 are sampled from these spectrograms.

We used a self-convoluted version of a Nuttall's window for calculating these spectrograms. It is the 12-th item of Table II of the reference [24]. This self-convoluted window has the maximum sidelobe level at -186.64 dB and 36 dB/oct decay rate. Low sidelobe level and steep decay rate of this window allow us to inspect low level spurious of the proposed procedure. The window length and frame shift were 40 ms and 2 ms respectively.

A.3. IIR equalizer design

The target equalizer shape is designed to equalize attenuation up to 68 dB for 6-term and 58 dB for 5-term cosine series, respectively. The FFT buffer length was 32768 and the length of the FIR response was 161 taps. The original equalizer shape, represented as an absolute spectrum, was converted to FIR response and truncated using one of Nuttall windows [24]. The 12-th item of Table II of the reference was used. It has the maximum sidelobe level of -93.32 dB and decay rate -18 dB/oct.

The IIR equalizer was designed using the auto correlation coefficients of this truncated FIR response, by applying LPC analysis. Figure 5 shows the frequency response of each equalizer and pole locations. The poles are not close to the unit circle, indicating numerical stability of the equalizers.

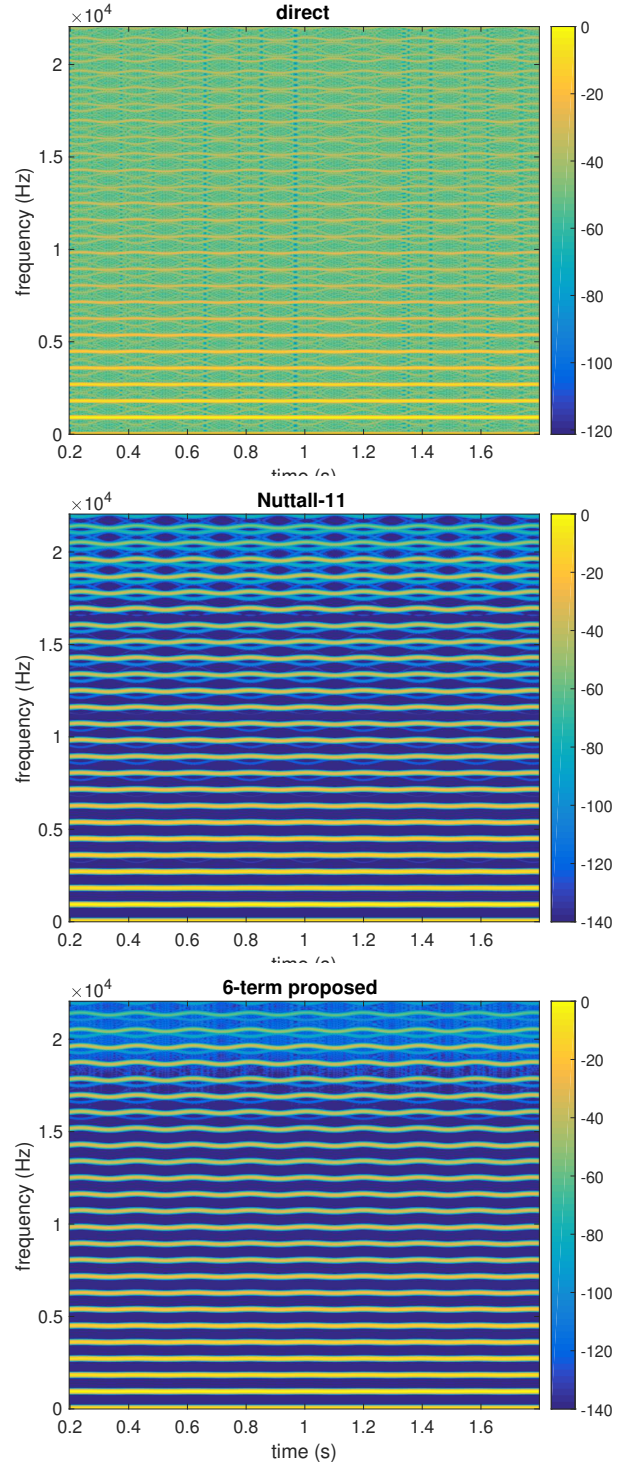


Figure 4: Spectrogram of direct discretization, antialiasing with Nuttall-11 window, and antialiasing with the proposed 6-term cosine series.

A.4. MATLAB functions

The following MATLAB functions are prepared to generate excitation source signals.

antiAliasedPolynomialSegmentR Generate a time

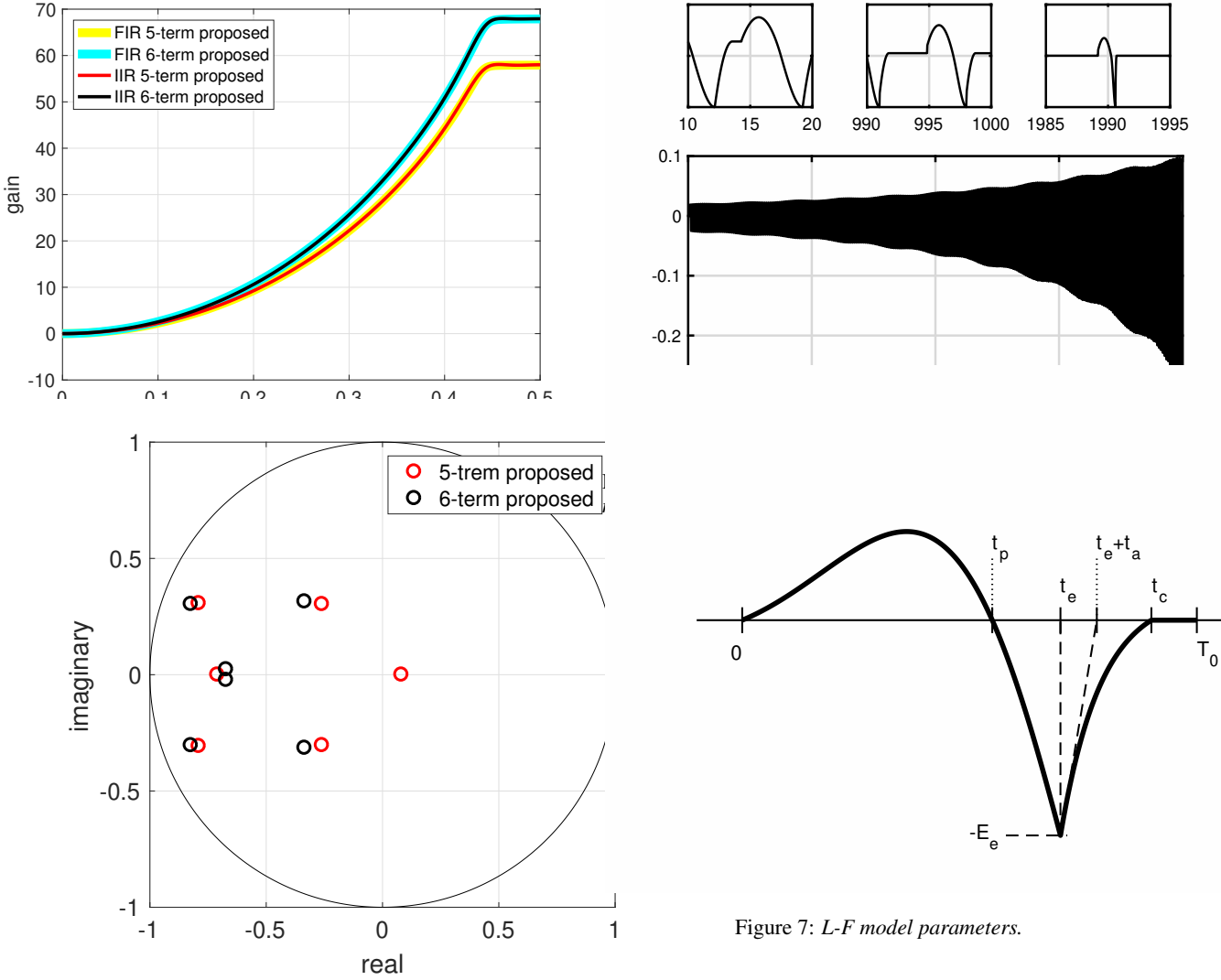


Figure 5: (upper plot) Frequency gain of equalizer using FIR implementation and IIR implementation. (Bottom plot) Pole locations of each equalizer. It also shows the unit circle on the complex plane.

normalized segment of an antialiased polynomial pulse.

antialiasedFIModelSingleR Generate one cycle of an antialiased F-L model excitation signal.

AAFjLjmodelFromFOTrajectoryR Generate an antialiased F-L model excitation signal using the given F0 trajectory and constant F-L model parameters.

AAFjLjmodelFromFOTrajectoryTVR Generate an antialiased F-L model excitation signal using the given F0 trajectory and time varying F-L model parameters.

We used **AAFjLjmodelFromFOTrajectoryR** to generate the test signal used to draw Figs. 3 and 4.

Figure 6 shows an example of an excitation signal with time varying F-L model parameters. The total airflow of each pitch cycle is kept constant.

A.5. Application to aliasing-free L-F model

Figure 7 shows the L-F model waveform with time parameters to define it. There is a typo in the L-F model definition given on the page 6 of the original reference [4], while other descriptions in the reference are correct. The fixed equation of defining the L-F model is as follows.

$$E(t) = E_0 e^{\alpha t} \sin \omega_g t \quad (t < t_e) \quad (40)$$

$$E(t) = \frac{-E_e}{\beta t_a} [e^{-\beta(t-t_e)} - e^{-\beta(t_c-t_e)}] \quad (t_e \leq t < t_c), \quad (41)$$

where $E(t)$ is defined as the time derivative of the glottal airflow $U_g(t)$. It is convenient to normalize time axis by T_0 and amplitude by E_e without losing generality. Then, the coefficients to be determined from the design parameters are E_0/E_e , α , ω_g and β . Since the airflow is zero while vocal fold is closing, the following constraint holds.

$$\int_0^{T_0} E(t) dt = 0. \quad (42)$$

The following steps provides the parameter values. First, Eq. 41 by substituting $t = t_c$. Then, using Eq. 42 and $\omega_g =$

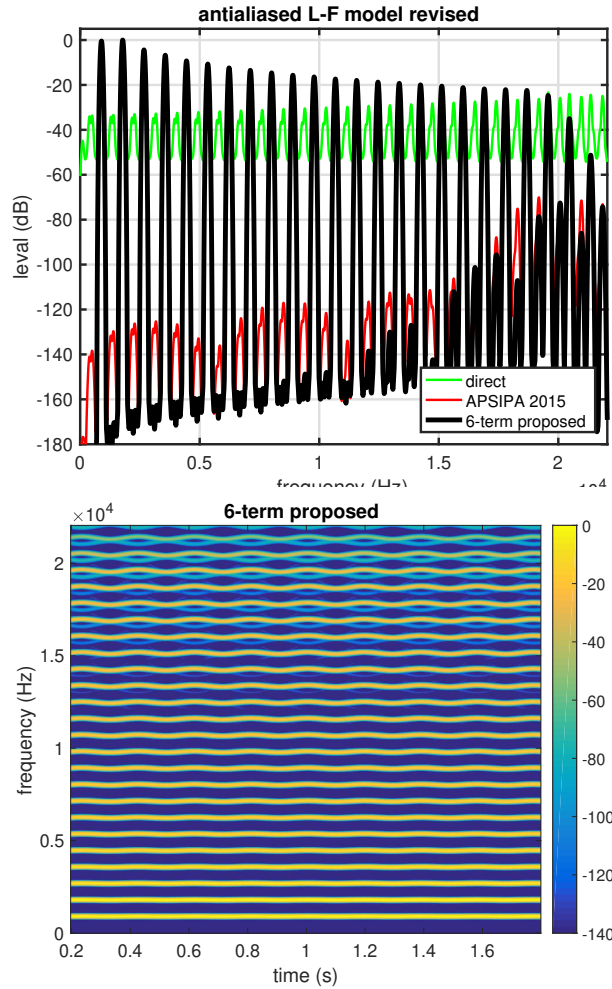


Figure 8: (Upper) Spectrum slice of direct discretization, our previous implementation, and antialiasing with the proposed 6-term cosine series. (Lower) Spectrogram.

t_p/π to determine α . We used numerical optimization function `fzero` of MATLAB to implement these.

A.5.1. Spectrum slice and spectrogram

Figure 8 shows spectrum slice and spectrogram of a generated test signal. The same frequency modulated F0 trajectory was used. Details are given in Appendix A.1